Journal of Metals, Materials and Minerals, Vol. 31, No. 2, pp. 1-9, 2021

Analysis of the impact factors from the friction stir welding process for dissimilar butt joints between semi-solid cast aluminum 356 and AISI 1018 carbon steel

Worapong BOONCHOUYTAN[1,*], Jaknarin CHATTHONG[1], and Rommadorn BURAPA[1]

[1] *Rajamangala University of Technology Srivijaya, Ratchadamnoennok Road, Muang, Songkhla 90000, Thailand*

***Corresponding author e-mail:** worapong.b@rmutsv.ac.th

Received date:
22 December 2020
Revised date
12 June 2021
Accepted date:
15 June 2021

Keywords:
Friction stir welding;
Dissimilar butt joints;
Semi-solid cast aluminum

Abstract

This research aimed to study the impacts of three different rotation speeds of 710, 1000, and 1400 rpm and three welding speeds of 40, 56, and 80 mm·min^{-1}, on dissimilar butt joints between semi-solid aluminum 356 and AISI 1018 carbon steel. Welding tools were made from tungsten carbide material, and the offset was 0 mm. It was found that an increase in the rotation speed and welding speed caused accumulated heat, which led to the appropriate changes in the metallurgical structure. The rotation speed and welding speed factors had the impact on the greater blending of the two metals at the SZ zone. A larger amount of semi-solid aluminum 356 infiltrated into the AISI 1018 carbon steel when the rotation speed and welding speed increased. The findings showed that the most influencing factors on the average tensile strength at the weld lines were the rotation speed of 1000 rpm and the welding speed of 56 mm·min^{-1}. The experiment in this study showed the maximum average tensile strength of 139.9 MPa and the average hardness value of 264.5 HV as the highest hardness value at the welding rotation speed of 1400 rpm and the welding speed of 80 mm·min^{-1}.

1. Introduction

Presently, there are problems concerning high-priced fuels and environmental issues. Thus, the automobile industry has invented and designed fuel-efficient cars which can maximize fuel economy. Moreover, these cars must not cause more pollution in order to help conserve the environment. The newly-designed cars need to give the highest performance according to customer's needs. With regard to the situations mentioned above, this research explores the possibility of using lightweight materials, such as aluminum, to replace some steel car parts to reduce the overall weight of the vehicles. Aluminum is a strong metal that has a higher strength-to-density ratio than steel. This ensures that the aluminum structure of the vehicle is sufficiently strong [1].

However, it is difficult to bridge aluminum and steel together because aluminum and steel have different physical-mechanical and chemical properties. Thus, when the materials are combined, problems often arise. For example, difference in elasticity modules causes the mechanical incompatibility and increases the stress concentration in the weld lines and stress discontinuities at the joint area. Also, the difference in thermal conductivity of aluminum and steel causes the different mechanisms of heat dissipation, resulting in thermal stresses that decrease the ability to resist to stress of the material [2]. The difference in chemical mixtures of the two materials causes inter-metallic compounds (IMCs), containing brittleness and is an important factor that reduces the strength of the weld lines. Therefore, finding the right welding process to join together aluminum and steel is a very important area of research to be continuously conducted.

Aluminum and steel condensations in any form result in semi-metallic compounds which can be divided into 5 types, including Fe_3Al, FeAl, $FeAl_2$, Fe_2Al_5, and $FeAl_3$. Also, they can be divided into 2 groups, based on the force support [3]. The first group contains high iron, i.e. Fe_3Al, and FeAl. Materials in this group have great resistance to corrosion, oxidization, and collapse. As a result, these materials are useful for automotive industry. Another group of materials contains high aluminum, including $FeAl_2$, Fe_2Al_5, and $FeAl_3$. These materials contain IMC and there are problems welding them together due to the hardness and brittleness issues. The ability to control IMC of the materials is important to improve the mechanical properties of the weld lines of steel and aluminum. Examples of IMC control can be found in research on mechanical formation of IMC using diffusion bonding [4].

The friction stir welding (FSW) is a solid-state welding invented by The Welding Institute (TWI) in England to weld materials that are difficult to weld together through the molten welding process, such as welding of aluminum alloys of different grades [5,6], and different materials that are needed to be joined together. The FSW process creates a fine grain welding structure, which can handle high loads and it is not possible to obtain this property using molten welding [7]. The FSW is very suitable method when melting of the materials is not needed to occur. The melting process may result in a change in microstructure from the cooling down of the liquid to solid, described by the principle of semi-solid cast aluminum alloy production. In addition, welding of semi-solid aluminum with mild steel is a very new technology. Little evidence has been found in the research database. Some experiments have been done on the friction stir welding between aluminum and steel, such as connecting aluminum 5186 with mild steel. The findings

showed that, at low welding speeds, the occurrence of IMC is characterized by Al_6Fe and Al_5Fe_2 at the weld lines, resulting in low strength values. In contrast, as welding speeds were set up at a higher level, the IMC formation decreases, resulting in higher strength values and reducing defects in the weld lines [8]. In welding of AA6181-T4 aluminum with HC260LA and DP600 steel, the formation of IMC is characterized by Fe_2Al_5 in the weld line. The strength of the weld lines can be increased up to 80% of aluminum strength [9]. Low level of welding rotation speed does not produce sufficient temperature for the cohesion of the two materials, and at a higher rotation speed, the temperature is very high, causing excessive burrs on the weld lines. The maximum strength of the weld lines in this experiment at the offset of +0.2 mm resulted a scattering of the steel in the aluminum matrix [10]. However, welding of aluminum alloy obtained by the semi-solid casting process, which is a new material with a circular grain structure, to steel using friction stir welding technique is a new technology. It has not yet yielded evidence from any research.

According to the abovementioned information, it has led the researchers to carry out this research project entitled friction stir welding of dissimilar joint semi-solid cast aluminum 356 (SSM 356) and carbon steel AISI 1018. This research aims to study the factors that affect the welds, i.e. rotation speed, welding speed, and the offset, examining changes in metallurgical properties (macro and micro-structure) and the specific mechanical properties of the welding stir zone and the thermos mechanical affected zone (TMAZ) in order to find appropriate macro, micro and mechanical characteristics. The results of this research can be useful in the selection of the appropriate welding methods in further research and industrial sector.

2. Materials and methods

The SSM 356 and AISI 1018 with a width of 50 mm, a length of 100 mm, and a thickness of 4 mm were used in this experiment. The chemical composition and mechanical properties of both experimental materials are shown in Table 1. The experiment located AISI 1018 carbon steel on the advancing side and the semi-solid cast aluminum 356 on the retreating side. At the beginning of welding process, the stirring shoulder was placed into the semi-solid cast aluminum 356 side and thrust towards the weld line. The surface of the stirring pinhead was thrust into the side of carbon steel AISI 1018, as shown in Figure 1(a). The offset distance is 0 mm as shown in Figure 1(b). The FSW welding tools which are the tool shoulder of a diameter of 20 mm and a pin stirring tool pin which has a diameter of 5 mm and a length of 3.2 mm were manufactured from tungsten carbide as shown in Figure 2. Based on the findings of previous research regarding the optimal offset [11], the factors of the friction stirring in this experiment were determined and are presented in Table 2. Before the welding experiment, the surface of the welding joint between the semi-solid cast aluminum and carbon steel was cleaned using acetone.

After welding, the specimen was cross-sectioned perpendicularly to the welding direction using Chen Long vertical band sawing machine (CS-230) in order to detect any occurring flaws and analyze metallurgical structure. The microstructure of the welding joint was examined by optical microscopy (OM) and scanning electron microscope (SEM). The hardness value of the same specimen used in the metallurgical structure analysis was examined using the Vikers method. The indenter was pressed on the cross-sectional area of the welding joint with a load of 100 kgf for 10 s. The distance between indentations was 1 mm. The specimen tensile strength was obtained from the force test on cross-sectioned specimen of stirring friction welding process according to ASTM E8M. The force test was performed by the Narin universal tester (NRI-TS501-100) at room temperature with a speed of 1 $mm \cdot min^{-1}$. Three specimens were tested for each welding experiment, and the average values were used to determine the tensile strength of the welding joints.

Table 1. The chemical mixtures of experimental material SSM 356 and AISI 1018.

Elements	**Si**	**Fe**	**Cu**	**Mn**	**Mg**	**Zn**	**Ti**	**Cr**	**Ni**	**Al**	
SSM 356	7.74	0.57	0.05	0.06	0.32	0.01	0.05	0.02	0.01	Balance	
Elements	**C**			**Mn**			**P**			**S**	**Fe**
AISI 1018	0.16-0.19			0.80			0.045			0.045	Balance

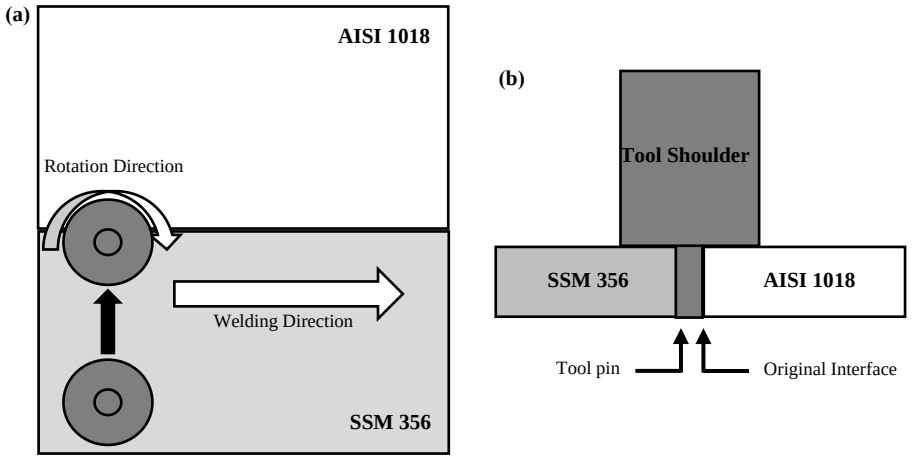

Figure 1. Shows the photograph of the experimental setup.

Table 2. Various factors for friction stirring butt welding of SSM 356 and AISI 1018.

Specimen no.	Rotation speed (rpm)	Welding speed ($mm \cdot min^{-1}$)	Number of welds (repeats)
FSW1	710	40	3
FSW2	710	56	3
FSW3	710	80	3
FSW4	1000	40	3
FSW5	1000	56	3
FSW6	1000	80	3
FSW7	1400	40	3
FSW8	1400	56	3
FSW9	1400	80	3

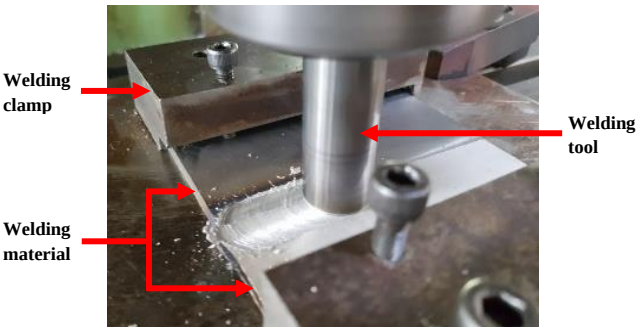

Figure 2. Friction stir welding process of SSM 356 and AISI 1018.

3. Results and discussion

3.1 Metallurgical structure of welding joints

The experimental material flow between the semi-solid cast aluminum 356 and AISI 1018 carbon steel varied; it could be noticed from the surface of the two welds, resulted from different welding factors as shown in Figure 3(a)-(i). The influence of friction stir welding factors was found in weld heat dissipation in the weld lines. In particular, the cooling of the two materials was completely different; the semi-solid aluminum 356 had a lower cooling rate than AISI 1018 carbon steel. Therefore, the flow of the experimental materials which were two different kinds of metals resulted in different surfaces of the welding joints. There were no defects such as cracks, fissures, or tunnels found in the welding joints. Regarding the rotation speed, it was found that the flow of the materials increased when the rotation speed increased. It was observed from the welding joints that the weaker material flew over the welding tool shoulder [12-14]. This can be caused by the great amount of heat transferring from the welding tool to both materials; semi-solid cast aluminum 356 received a higher heat content than carbon steel AISI 1018, resulting in more flanges on the side of semi-solid cast aluminum 356. Additionally, it was found that a reduction in the welding speed allowed the observation of the increased material flow and consistent mixing. The formation of flanges appeared on the aluminum side when the two different materials were welded together. The top surface of the welds were compared and shown in Figure 3(a) and 3(c).

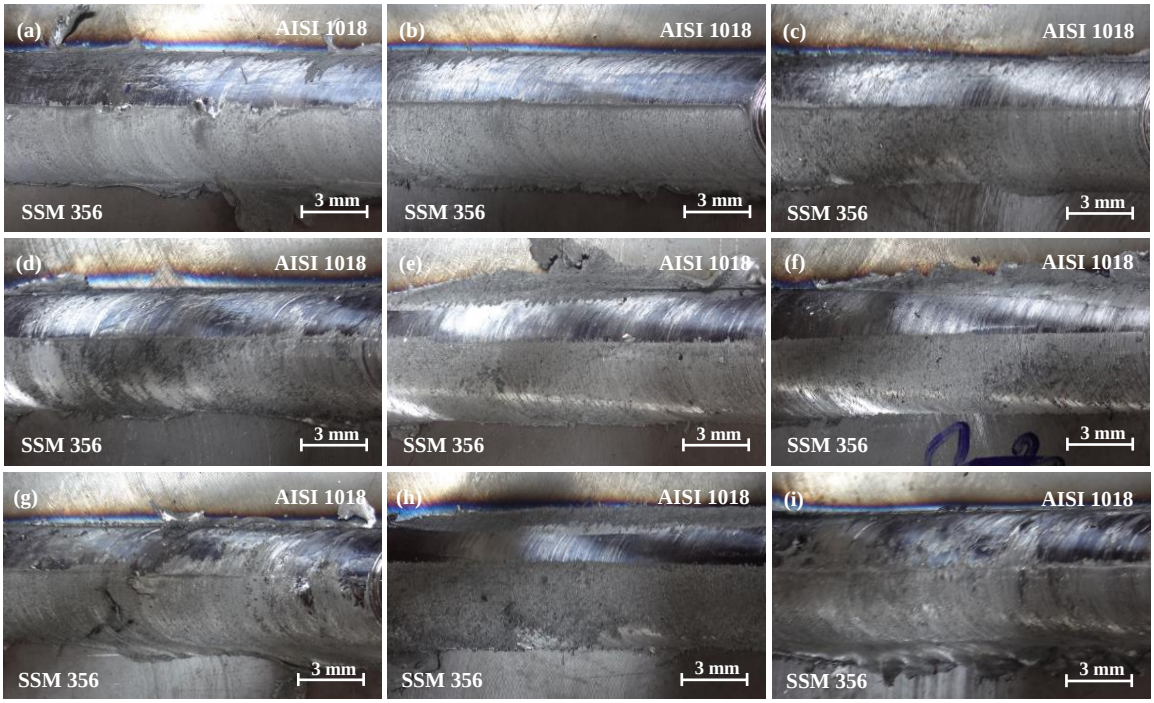

Figure 3. The top surface of the weld for (a) FSW1, (b) FSW2, (c) FSW3, (d) FSW4, (e) FSW5, (f) FSW6, (g) FSW7, (h) FSW8, and (i) FSW9.

3.2 Macro and microstructure of welding joints

Figure 4 shows the different macrostructures and microstructures of the welding joints which were resulted from factors in the stirring friction welding process. Different regions of the welds, such as the original metal texture or Base Metal (BM), Heat-affected Zone (HAZ), Thermo-Mechanical Affected Zone (TMAZ) and the Weld Zone (Stir Zone: SZ) were examined using a microscope.

The results showed that the formation of narrow HAZ and TMAZ regions was observed on both semi-solid cast aluminum 356 and AISI 1018 carbon steel metals. It was found in the experiment that the proposed rotation speeds and welding speeds resulted in different region shapes due to the rapid cooling from the maximum temperature to the cooler air. In particular, the microstructures in the TMAZ and the SZ regions were largely subjected to plastic deformation, which was a direct impact of welding tools. The welding tools also made the grain in both regions significantly different than the others. These occurrences could result from the welding factors; an increase in the welding factors, i.e. welding rotation speed and welding speed, affected the heat conductivity of the welds [15,16]. The most relevant mechanisms for mechanical deformation were dynamic recovery (DRV), continuous dynamic recrystallization (CDRX), intermittent dynamic crystallization (DDRX), and geometric dynamic recrystallization (GDRX), depending on the energy transfer efficiency of the materials [17]. Besides, the friction stir welding process affected the structure of grains in the TMAZ region and SZ regions during severe plastic deformation of the process. Later, the rapid cooling from the maximum temperature after the welding process also caused the grain to deform, and the dislocation of grain boundary led to the formation of the same grain structure in the SZ in the welding joints in both sides of semi-solid aluminum 356 and AISI 1018 carbon steel. The greater size of grain in the narrow HAZ can be observed from the semi-solid cast aluminum 356 side. Although the grain structure in the TMAZ region of both semi-solid cast aluminum 356 and AISI 1018 carbon steel sides was scattered according to the welding tool rotation direction due to the shear force caused by the welding tool's rotation during welding, there were no obvious signs of welding defects at the macrostructure level in the friction stir welding experiment.

Regarding the microstructure, the changes in rotation speed and welding speed were seen to affect the metal fusion in the SZ area. The semi-solid cast aluminum 356 was better blended into the AISI 1018 carbon steel as the rotation speed and welding speed increased. This could be explained by the fact that the welding heat was accumulated and transferred to the weld, resulting in a sufficient heat to cause the fusion between the two materials. How the two metals mixed were compared and shown in Figure 4(a)-(c) and 4(g)-(i). In addition, the increased shear stress arising from the welding tool's rotation speed made the AISI 1018 carbon steel material more malleable. As a result, the semi-solid cast aluminum 356 infiltrated and blended better with the AISI 1018 carbon steel, resulting in the increased strength of welding joints. On the other hand, the low rotation speed generated less accumulated heat in the welding zone. Hence, the semi-solid cast aluminum 356 was not mixed well with the AISI 1018 carbon steel, as presented in Figure 4(a)-(c).

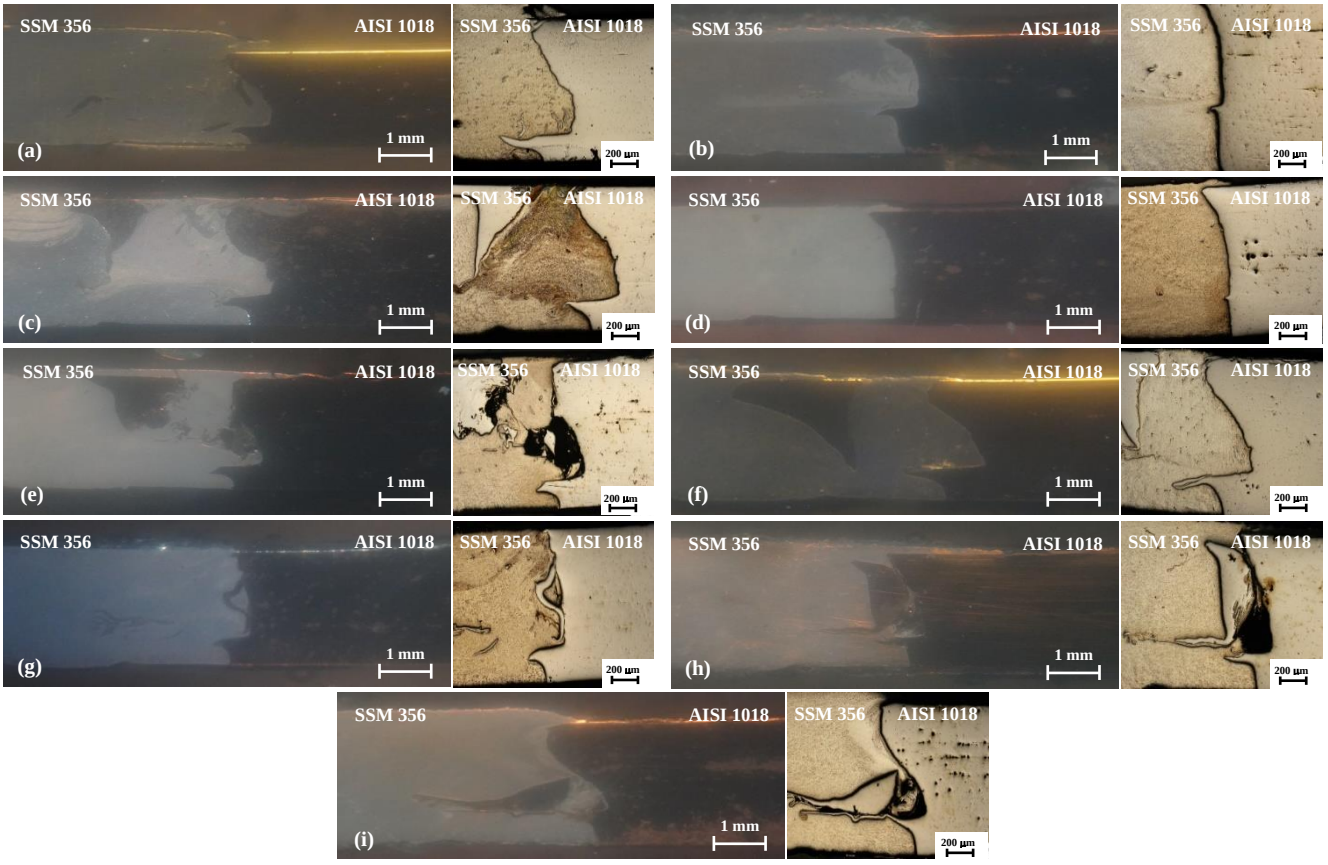

Figure 4. Macro and micro structures of the weld for (a) FSW1, (b) FSW4, (c) FSW7, (d) FSW2, (e) FSW5, (f) FSW8, (g) FSW3, (h) FSW6, and (i) FSW9.

An important observation is that AISI 1018 broke into large-sized particles which scattered in the SZ when the lower welding speed was used. When the welding speed increased at a speed higher than 40 mm·min^{-1}, the welding surface was generally smoother and lighter. The process gave the smoothest welding surface when the welding speed of 56 mm·min^{-1} was performed. This speed parameter, when operated together with the rotation speed at 1000 rpm, gave the optimum welding performance. Moreover, there were no defects, such as cracks or voids, found in the SZ when macrostructure testing was carried out. These findings are in line with the findings of previous welding research [14].

The scanning electron microscopy (SEM) of microstructures of the welds which were conducted with the rotation speed of 1400 rpm and the welding speed of 80 mm·min^{-1} was selected to particularly examine in this study. The formation of a thin layer of intermetallic compounds (IMCs) between the semi- solid cast aluminum 356 and the welded AISI 1018 carbon steel could be noticed. The thickness of the IMC layer (With pointing arrows) varied, depending on the rotation speed and welding speed of the welding tool, which caused the friction of the tool and heat. The important fact is that the formation of a wavy interface under the influence of pinhead rotation in the welding region caused the intensifying mechanical coordination [14], deformation in the interface area, and the formation of intermetallic layers in the welding zone. These properties altogether resulted in the desirable welding joints.

The shape of the grains and the phase compositions in the SZ was found in lamellar structure. Thick intermetallic layer was formed at the Al/Fe interface. It can be assumed that the flow of the metals was a result of the high speed of stir rotation of the welding tool during the process. These findings were similar to the observations in [18].

Figure 5 presents the infiltration of semi-solid aluminum 356 into the AISI 1018 carbon steel side, caused by the rotation speed and welding speed factors. The energy dispersive X-Ray (EDX) examination was carried out and the results showed that the chemical mixtures of the welds contained 52.2% of Al, 39.1% of Fe, and 8.7% of Si, as shown in Figure 6.

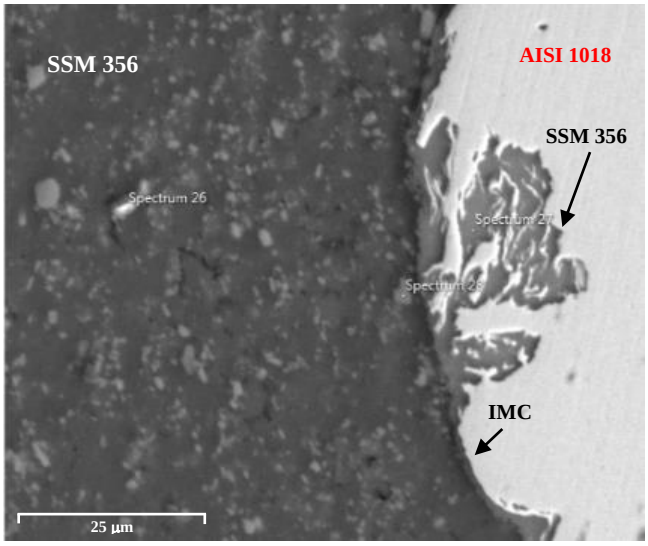

Figure 5. The SEM microstructure weld at a rotation speed of 1400 rpm and welding speed of 80 mm·min^{-1}.

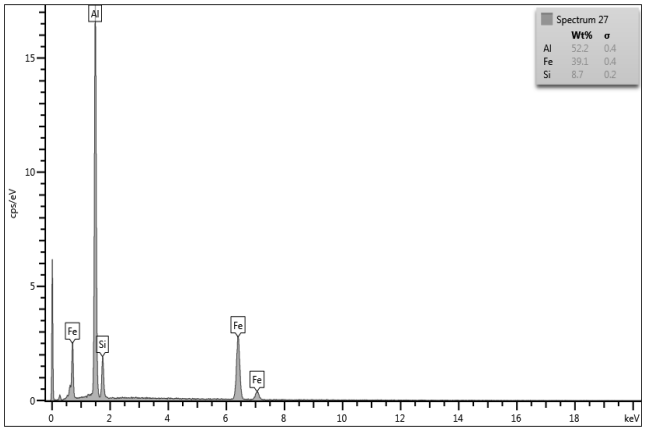

Figure 6. The EDX weld at a rotation speed of 1400 rpm and welding speed of 80 mm·min^{-1}.

3.3 The tensile strength of the welds

The tensile strength test results showed that the accumulated heat from the semi-solid cast aluminum 356 welding was transmitted to the AISI 1018 carbon steel side because the tool's rotation speed made the material flow through the tool and the welded metal, and caused heat to generate from welding friction. It generated welding heat from friction stirring, which is the main influence for plastic deformation. Welding performance could be observed from the adhesion of the two materials. For instance, a welding rotation speed of 710 rpm and a welding speed of 80 mm·min^{-1} achieved the tensile strength mean of 107.3 MPa, which was the lowest value in this trial, resulting from over speeding in stir welding; the heat was not yet accumulated much in the welding process. Hence, the adhesion of the semi-solid cast aluminum 356 to the AISI 1018 carbon steel was not complete. On the other hand, the increasing rotation speed gave the greater tensile strength. For instance, a welding rotation speed of 1000 rpm and a welding speed of 56 mm·min^{-1} yield the mean tensile strength of 139.9 MPa, which was the highest value in this experiment. In this welding condition, the greater combination between the materials was observed; the macro-micro structures demonstrated that the mechanical characteristics of tensile strength improved. Besides, the comparison of the welding performance with the original metal materials showed that the tensile hardness value of the welds was 66.84% greater than that of the semi-solid aluminum 356, and 30.57% greater than that of the original AISI 1018 carbon steel as it was shown in Table 3.

The findings indicated that the rotation speed and welding speed factors were the main priorities in friction stir welding which generate the heat by friction between the welding tool and the welded metals. Furthermore, the heat transferred to the welded materials, plasticized them, and caused them to adhere to each other. These factors influenced the welding process, i.e. improving the quality of the welds, increasing the adhesion of the welds, and reducing the deformation in the interface area and the intermetallic layer formation at the welding zone.

Figure 7 shows the comparison of the tensile strength of friction stir welding factors, namely rotation speeds of 710, 1000, and 1400 rpm. It was found that the welding speed of 56 mm·min^{-1} yielded the highest tensile strength among the examined rotation speeds. This phenomenon

Table 3. The tensile strength of weld for SSM 356 and AISI 1018.

Factor		Tensile strength (MPa)	Yield strength (MPa)	Elongation (%)	Joint efficiency (SSM 356) (%)	Joint efficiency (AISI 1018) (%)
Base SSM 356		187.20	124.90	8.90	-	-
Base AISI 1018		409.10	285.20	29.80	-	-
710	40	109.80	87.80	0.40	58.70	26.80
	56	134.70	107.80	0.80	72.00	32.90
	80	107.30	85.80	0.60	57.30	26.20
1000	40	134.30	107.40	1.10	71.70	32.80
	56	139.90	111.90	0.50	74.70	34.20
	80	121.90	97.50	0.40	65.10	29.80
1400	40	120.30	96.20	0.40	64.30	29.40
	56	131.10	104.90	1.60	70.00	32.00
	80	127.00	101.60	1.50	67.80	31.00
Average					66.84	30.56

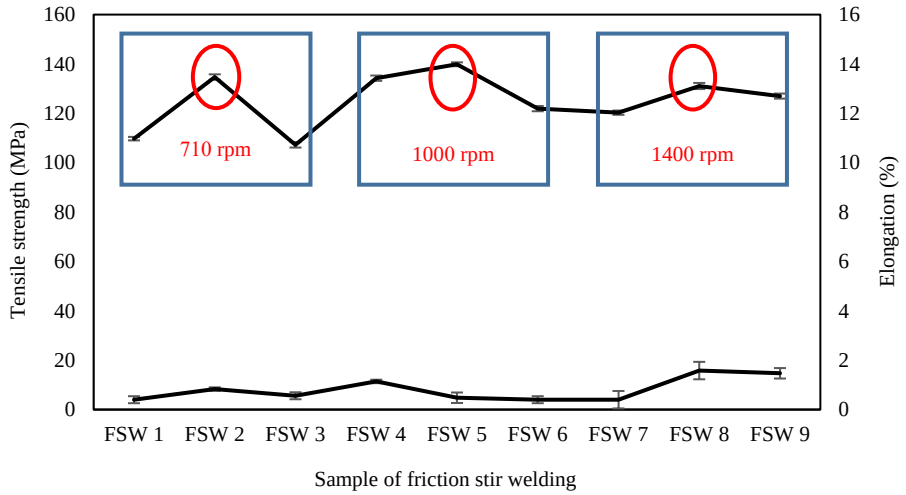

Figure 7. Comparison of tensile strength for each friction welding factor.

was caused by the friction process between the metals and the complete welding direction, the optimal plastic deformation, and the appropriate welding rotation speed that assisted the material flow onto the AISI 1018 carbon steel. It was also observed that the welding speed of 80 mm·min^{-1} resulted in the lower tensile strength compared to other welding speeds. This could be explained by the insufficient heat from the welding process that did not cause the proper plastic deformation, an important condition that leads to incomplete precipitation of the various phases and low tensile strength. It was shown that the elongation percentage during the whole experiments was less than 2% due to the sudden fractures (Brittle fracture) of the metal samples, which showed that the specimens were not connected properly, as presented in Figure 8(a) and 8(b). The brittle fracture of two-metal joins occurred because the aluminum and steel metals did not blend into each other properly. If the dissipation or bond between aluminum and steel atoms improves, the elongation and tensile strength will increase [19].

The tensile test of the weld joints performed at different rotation speeds has shown that the joints resulted from the lowest rotation speed (710 rpm) cracked in the SZ as illustrated in Figure 8. The joints performed at any speed higher than 710 rpm tended to crack in TMAZ in the side of the AISI1018 or near the interface. The welding speed at 56 mm·min^{-1} also resulted in the highest tensile strengths in all sets of examined rotation speed parameter, with the average joint efficiency at 35.6%. Based on the examination of the welding parameters in this study, it was noticed that the fracture always occurred opposite the Al/Fe interface. Moreover, this study revealed differentiated characteristics of fracture surface and clearly described the ductile-brittle fracture mechanisms in relation to the examined FSW parameters. In this study, ductile-brittle combination did not appear to significantly affect the occurrence of fracture since the strong welding pressure was not applied and the severe formation of welding dents was not observed [20,21].

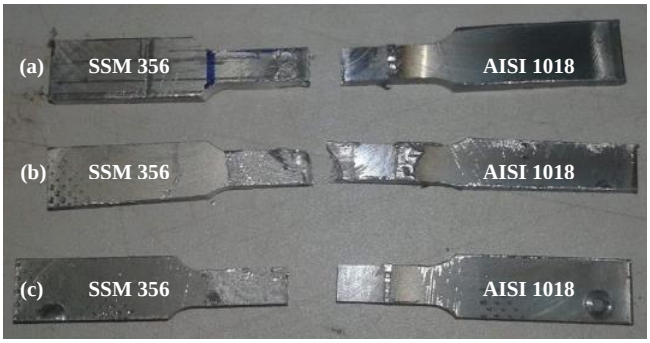

Figure 8. The tensile strength test of specimen fracture (a) rotation speed of 710 rpm, (b) rotation speed of 1000 rpm, and (c) rotation speed of 1400 rpm.

3.4 The hardness values of welding joints

The average of hardness test results of the friction stir welding joints of dissimilar materials between SSM 356 and AISI 1018 were shown in Figures 9-11.

The average hardness value of the welds conducted with a rotation speed of 710 rpm, welding speeds of 40, 56, and 80 mm·min^{-1} are shown in Figure 9. It was found that the highest average hardness at the SZ region was 165.5 HV at a welding speed of 80 mm·min^{-1}, and the minimum average hardness was 115.9 HV at a welding speed of 40 mm·min^{-1}.

The average weld hardness at the rotation speed of 1000 rpm, the welding speeds of 40, 56, and 80 mm·min^{-1} are shown in Figure 10. The obtained results showed that the highest average hardness at the SZ region was 238.2 HV, at the welding speed of 80 mm·min^{-1}. The minimum average hardness was 214.3 HV, at the welding speed of 40 mm·min^{-1}.

The average weld hardness at the rotation speed of 1400 rpm, the welding speeds of 40, 56, and 80 mm·min^{-1} are shown in Figure 11. The obtained results showed that the highest average hardness at the SZ region was 264.7 HV, at the welding speed of 80 mm·min^{-1}. The minimum average hardness was 247.3 HV, at the welding speed of 40 mm·min^{-1}.

The emerging pattern of the weld hardness in the experiment showed that the hardness values in the two sides of the welds varied. From the center of the welds at the SZ region, the tendency of asymmetric hardness of the two metals was observed due to the different physical and mechanical characteristics of the two dissimilar experimental materials. The findings indicated that the centerline hardness value was the highest for each rotation speed factor. This hardness was greatly affected by microstructure modification resulted from the rapid cooling of the materials, the rapid change in grain size, and the formation of an IMC layer between the two metals [14]. In addition, the weld hardness gradually reduced from the SZ region down to the base hardness of the experimental metals. This was affected by the tool's welding rotation that continuously transferred the high heat to the SZ region and distributed the heat to the TMAZ and the HAZ areas. Therefore, the grains in the area distant from the joints were less affected; there was little change in the grain size and little chance of plastic deformation in the area distant from the joints. These inevitably caused the strength value of the two metals not to change much.

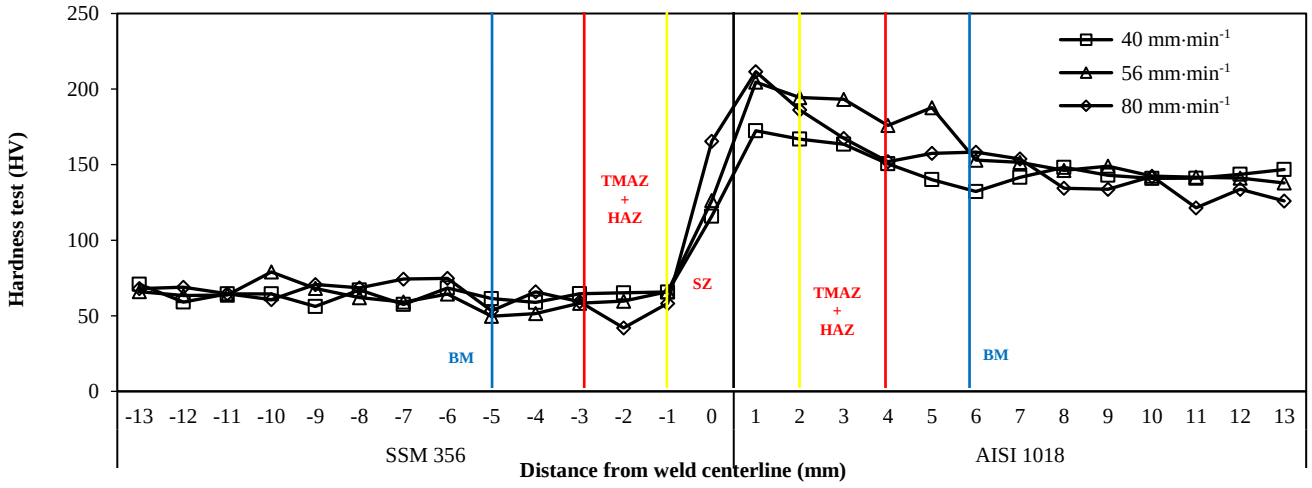

Figure 9. The weld hardness at a rotation speed of 710 rpm.

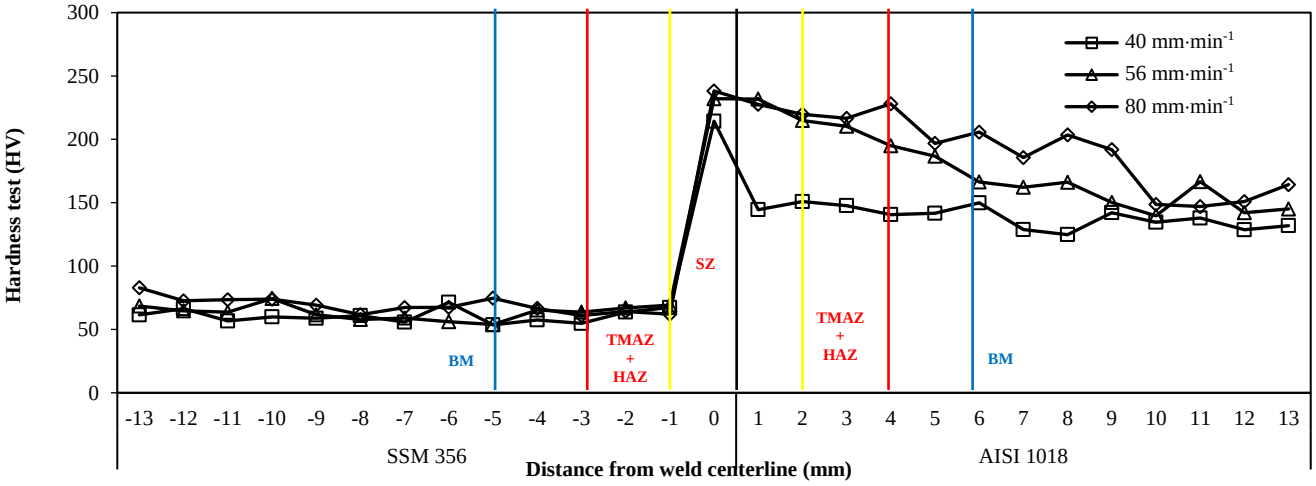

Figure 10. The weld hardness at a rotation speed of 1000 rpm.

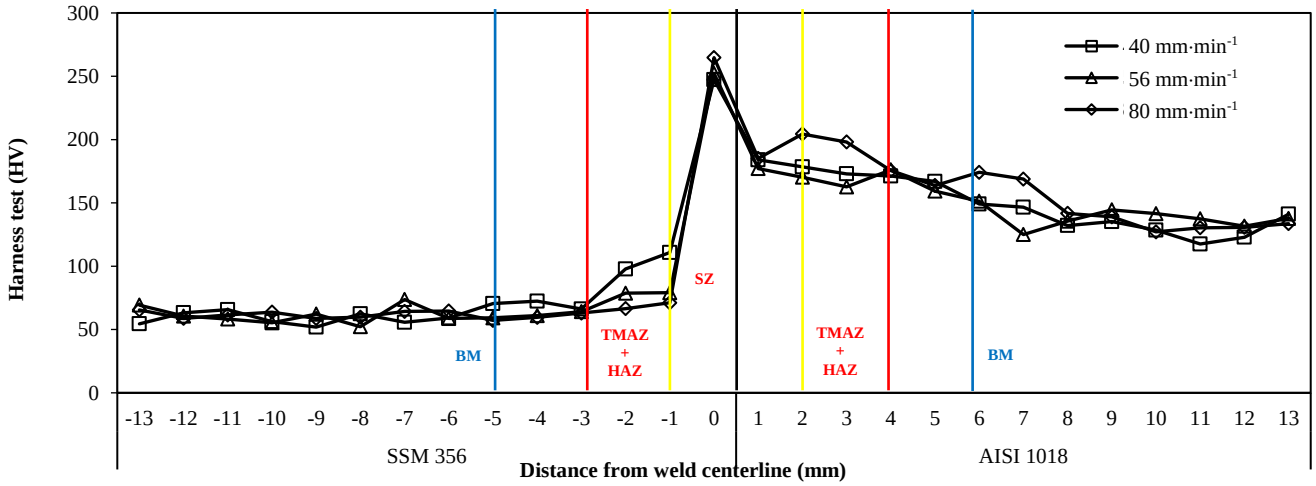

Figure 11. The weld hardness at a rotation speed of 1400 rpm.

4. Conclusions

The appropriate increase in rotation speeds and welding speeds caused accumulated heat in the welding joints, which led to a suitable change in the metallurgical structure.

The friction heat of the welding tool and the experimental materials at the welding zone caused the materials flow in the form of plastic deformation at the welding edge, and the heat was distributed to different areas of the welding zone.

The rotation speeds and welding speeds affected the fusion of the two metals at the SZ region; a greater amount of SSM 356 was pressed into AISI 1018 when the welding rotation speed and the welding speed increased.

The most influencing factors on the average tensile strength of the welds were the welding rotation speed of 1000 rpm and the welding speed of 56 mm·min^{-1}. The welds produced under these speed conditions achieved the maximum average tensile strength of 139.9 MPa.

The highest average hardness of 264.7 HV was achieved in this experiment, performed with the rotation speed of 1400 rpm and the welding speed of 80 mm·min^{-1}.

Acknowledgements

This research was funded by the Rajamangala University of Technology Srivijaya.

References

[1] K. Kimapong, and T. Watanabe, " Friction stir welding of aluminum alloy to steel", *Welding Journal*, vol. 83(10), pp. 277S-282S, 2004.

[2] D. Brandon, and W. D. Kaplan, *Joining Processes: An Introduction.* New York: John Wiley & Sons, 1997.

[3] S. Kobayashi, and T. Yakou, "Control of intermetallic compound layers at interface between steel and aluminum by diffusion-treatment", *Materials Science and Engineering A*, vol. 338(1-2), pp. 44-53, 2002.

[4] T. B. Massalski, H. Okamoto, P. R. Subramanian, and L. Kacprzak, *Binary Alloy Phase Diagrams*, 2 nd Edition. OHIO: ASM International, 1990.

[5] W. M. Thomas, E. D. Nicholas, J. C. Needham, M. G. Murch, S. P. Temple, and C. J. Dawes, "Friction stir butt welding", *International Patent application*, No. PCT/GB92/02203, 1991.

[6] W. M. Thomas, and E. D.Nicholas, "Friction Stir Welding for the Transportation Industries", *Materials and Design*, vol. 18, pp. 269-273, 1991.

[7] R. S. Mishra, and Z. Y. Ma, "Friction stir welding and processing", *Materials Science and Engineering*, vol. 50(1-2), pp. 1-78, 2005.

[8] M. Dehghani, A. Amadeh, and M. S. A. A. Akbari, "Investigations on the effects of friction stir welding parameters on intermetallic and defect formation in joining aluminum alloy to mild steel", *Materials and Design*, vol. 49, pp. 433-441, 2013.

[9] R. S. Coelho, A. Kostkac, J. F. D. Santos, and A. R. Kaysser-Pyzalla, "Friction-stir dissimilar welding of aluminum alloy to high strength steels: Mechanical properties and their relation to microstructure", *Materials Science and Engineering A*, vol. 556, pp. 175-183, 2012.

[10] W. Takehiko, T. Hirofumi, and Y. Atsushi, "Joining of aluminum alloy to steel by friction stir welding", *Journal of Materials Processing Technology*, vol. 178(1-3), pp. 342-349, 2006.

[11] W. Boonchouytan, J. Chatthong, and R. Burapa, "Study the basic parameters of friction stir welding of dissimilar joint between aluminum alloy semi-solid metal 356 and mild steel", *Proceedings of Rajamangala Manufacturing & Management Technology Conference, Krabi, Thailand*, 2018, pp. 241-249.

[12] S. Zandsalimi, A. Heidarzadeh, and T. Saeid, "Dissimilar friction-stir welding of 430 stainless steel and 6061 aluminum alloy: Microstructure and mechanical properties of the joints", *Journal of Materials Design and Applications*, vol. 223(9), pp. 1791-1801, 2019.

[13] M. Habibnia, M. Shakeri, S. Nourouzi, and M. K. Besharati Givi, "Microstructural and mechanical properties of friction stir welded 5050 Al alloy and 304 stainless steel plates", *The International Journal of Advanced Manufacturing Technology*, vol. 76, pp. 819-829, 2015.

[14] E. Arameh, H. Abdelmagid, T. Faris, A. D. Hamed, and K. Farzad, "Simulation and experimental study of underwater dissimilar friction-stir welding between aluminum and steel", *Journal of Materials Research and Technology*, vol. 9(3), pp. 3767-3781, 2020.

[15] F. Khodabakhshi, A. P. Gerlich, A. Simchi, and A. H. Kokabi, "Cryogenicfriction-stir processing of ultrafine-grained Al–Mg–TiO_2 nanocomposites", *Materials Science and Engineering A*, vol. 620, pp. 471-482, 2015.

[16] F. Khodabakhshi, M. Nosko, and A. P. Gerlich, "Dynamic restoration and crystallographic texture of a friction-stir processed Al–Mg–SiC surface nanocomposite", *Journal Materials Science and Technology*, vol. 34(14), pp. 1773-1791, 2018.

[17] R. M. Terry, S. Srinivasan, and J. Q. Su, "Recrystallization mechanisms during friction stir welding/processing of aluminum alloys", *Scripta Materialia*, vol. 58(5), pp. 349-354, 2008.

[18] H. Y. Huang, I. C Kuo, and C. W. Zhang, "Friction-stir welding of aluminum alloy with an iron-based metal as reinforcing material", *Science and Engineering of Composite Materials*, vol. 25(1), pp.123-131, 2018.

[19] G. S. Sajin, "Friction stir welding of aluminum 6082 with mild steel and its joint analyses", M.D. thesis, Department of Materials Science and Engineering, Indian Institute of Technology Hyderabad, Telangana, India, 2012.

[20] S. Lia, Y. Chena, J. Kang, Y. Huang, J. A. Gianetto, and L. Yin, "Interfacial microstructures and mechanical properties of dissimilar titanium alloy and steel friction stir butt-welds", *Journal of Manufacturing Processes*, vol. 40, pp. 160-168, 2019.

[21] A. Eyvazian, A. Hamouda, F. Tarlochan, H. A. Derazkola, and F. Khodabakhshi, "Simulation and experimental study of underwater dissimilar friction-stir welding between aluminium and steel", *Journal of Materials Research and Technology*, vol. 9(3), pp. 3767-3781, 2020.